Journal of The Electrochemical Society, **162** (14) A2628-A2634 (2015)
0013-4651/2015/162(14)/A2628/7/$33.00 © The Electrochemical Society

Composite Gel Electrolytes for Suppressing Lithium Dendrite Growth and Improving Cycling Performance of $LiNi_{0.5}Mn_{1.5}O_4$ Electrodes

Won-Kyung Shin,[a] Se-Mi Park,[a,b] Yoon-Sung Lee,[c] and Dong-Won Kim[a,*,z]

[a]*Department of Chemical Engineering, Hanyang University, Seungdong-gu, Seoul 133-791, Korea*
[b]*Batteries R&D, LG Chem Ltd., Yuseong-gu, Daejeon 305-738, Korea*
[c]*Center for Energy Convergence, Korea Institute of Science and Technology, Seongbuk-gu, Seoul 136-791, Korea*

Core-shell structured SiO_2 particles with a poly(lithium acrylate) shell were synthesized and used in preparing a composite gel electrolyte. The composite gel electrolyte exhibited high ionic conductivity and favorable interfacial characteristics at the lithium electrode. The use of a composite gel electrolyte containing $SiO_2(Li^+)$ particles effectively suppressed both the dendrite growth of lithium and dissolution of transition metals from the active $LiNi_{0.5}Mn_{1.5}O_4$ material. The lithium metal polymer cell composed of a lithium negative electrode and a $LiNi_{0.5}Mn_{1.5}O_4$ positive electrode delivered a high discharge capacity of 136.6 mAh g^{-1} and exhibited good capacity retention.

Manuscript submitted August 5, 2015; revised manuscript received September 10, 2015. Published September 25, 2015.

Rechargeable lithium batteries using lithium metal as a negative electrode have attracted significant attention for use in high energy density power sources, because the lithium negative electrode can provide high specific capacity (3,862 mAh g^{-1}).[1] However, the use of lithium metal is still challenging because of the safety issues caused by lithium dendrite growth during repeated charge and discharge cycles.[2,3] In addition to the poor cycling stability, the flammable nature of liquid electrolyte based on alkyl carbonates can result in catastrophic failure.[4] Therefore, safer and more reliable electrolyte systems for use with lithium electrode are required, and polymer electrolytes are promising candidates in this regard.[5–7] Solid polymer electrolytes are ideal for use in lithium metal batteries; however, their low ionic conductivities (below 10^{-5} S cm^{-1} at ambient temperatures) limit their use. Accordingly, much research has focused on the preparation and characterization of gel polymer electrolytes that exhibit high ionic conductivities at room temperature.[8,9] In our previous study, composite gel electrolytes based on core-shell structured SiO_2 particles containing a poly(lithium acrylate) shell were applied to lithium-ion polymer cells composed of a graphite negative electrode and a $LiNi_{0.6}Co_{0.2}Mn_{0.2}O_2$ positive electrode.[10] The cells employing these composite gel electrolytes were characterized by high discharge capacity, good high rate performance and good cycling stability. In light of this previous study, we hypothesized that a composite gel electrolyte could suppress the formation and growth of lithium dendrites in lithium metal-based polymer cells.

In order to achieve high energy density, many research groups have developed high voltage cathode materials with high reversible capacities.[11] In particular, a spinel-structured $LiNi_{0.5}Mn_{1.5}O_4$ material has been of great interest because of its high theoretical capacity (147 mAh g^{-1}), high operating voltage and good rate capability.[12–15] However, dissolution of transition metals (Mn, Ni) into the electrolyte solution occurs when using $LiNi_{0.5}Mn_{1.5}O_4$ at elevated temperatures, and this dissolution can lead to a gradual deterioration of cell performance upon cycling. Numerous approaches to solve these problems have been proposed, including the use of new electrolyte systems, the addition of various additives to the electrolyte, and surface modification of active $LiNi_{0.5}Mn_{1.5}O_4$ materials.[16–21] The use of a composite gel electrolyte based on a core-shell structured SiO_2 is of our interest because the dissolution of transition metals in $LiNi_{0.5}Mn_{1.5}O_4$ is mainly caused by HF attack, and the SiO_2 particles can serve as HF scavengers to remove HF in the electrolyte.[22]

In this work, we prepared composite gel electrolyte based on poly(vinylidene fluoride-co-hexafluoropropylene) (P(VdF-co-HFP)) and core-shell structured SiO_2 particles containing poly(lithium acrylate). Lithium metal polymer cells employing a lithium negative electrode, a composite gel electrolyte and a $LiNi_{0.5}Mn_{1.5}O_4$ positive electrode were assembled, and their cycling performance was evaluated. Our results confirm that the use of a composite gel electrolyte containing $SiO_2(Li^+)$ particles was very effective in suppressing both the growth of lithium dendrites and the dissolution of transition metals from $LiNi_{0.5}Mn_{1.5}O_4$ resulting in good cycling performance of $Li/LiNi_{0.5}Mn_{1.5}O_4$ cells.

Experimental

Preparation of composite gel electrolyte.— Core-shell structured $SiO_2(Li^+)$ particles containing poly(lithium acrylate) in the shell were synthesized according to our previous work.[10] The $SiO_2(Li^+)$ particles were obtained as a fine white powder. A composite polymer film consisting of P(VdF-co-HFP) (Kynar 2801, Mw = 380,000) and $SiO_2(Li^+)$ particles was prepared by mixing P(VdF-*co*-HFP), $SiO_2(Li^+)$ particles and dibutyl phthalate (DBP) in acetone. The mixture was then ball milled and subsequent casting using a doctor blade. To form pores in the composite polymer membrane, the resulting film was immersed in methanol to remove the DBP and was then vacuum dried at 70°C for 12 h. The content of $SiO_2(Li^+)$ particles in the composite polymer membrane was maintained to 4.0 wt%, since the ionic conductivity was the highest at 4.0 wt% $SiO_2(Li^+)$.[10] Composite gel electrolyte was finally obtained by soaking the membrane in the liquid electrolyte consisting of 1.15 M $LiPF_6$ in ethylene carbonate (EC)/ethylmethyl carbonate (EMC)/diethyl carbonate (DEC) solution (3:5:2 by volume, battery grade, PANAX ETEC Co. Ltd.). Finally, the composite gel electrolyte was obtained as a freestanding film with a thickness of 25 μm. A composite gel electrolyte was also prepared as a control sample according to the same procedure, with $SiO_2(Li^+)$ being replaced by fumed silica.

$Li/LiNi_{0.5}Mn_{1.5}O_4$ cell assembly.— The positive electrode was prepared by coating a N-methyl pyrrolidone (NMP)-based slurry containing $LiNi_{0.5}Mn_{1.5}O_4$, poly(vinylidene fluoride) (PVdF) and super-P carbon (MMM Co.) (85:7.5:7.5 by weight) onto aluminum foil. The active mass loading in the positive electrode corresponded to a capacity of 1.6 mAh cm^{-2}. The negative electrode consisted of lithium metal (Honjo Metal Co. Ltd.) that was pressed onto a copper current collector. A CR2032-type coin cell was assembled by sandwiching the composite gel electrolyte between the lithium negative electrode and the $LiNi_{0.5}Mn_{1.5}O_4$ positive electrode. For comparison, a liquid electrolyte-based cell was also assembled with a polypropylene (PP) separator (Celgard 2400) and the same liquid electrolyte. All cells were assembled in a dry box filled with argon gas.

Characterization and measurements.— The morphology of the silica core particles was examined using a field emission scanning

*Electrochemical Society Active Member.
[z]E-mail: dongwonkim@hanyang.ac.kr

electron microscope (FE-SEM, JEOL JSM-6330F). Fourier transform infrared (FT-IR) spectra were recorded on a Magna IR 760 spectrometer with KBr powder-pressed pellets. The core-shell structured $SiO_2(Li^+)$ particles were characterized using a field emission transmission electron microscope (FE-TEM, FEI JEM 2100F). In order to measure the electrolyte uptake, the composite polymer membranes were immersed in a 1.15 M $LiPF_6$ solution in EC/EMC/DEC for 1 h. The membranes were taken out of the electrolyte solution, and the electrolyte uptake was then determined by using Equation 1,

$$\text{Uptake } (\%) = (W - W_o)/W_o \times 100 \quad [1]$$

where W_o and W are the weights of the membrane before and after soaking in the liquid electrolyte, respectively. AC impedance measurements were performed to measure ionic conductivity and interfacial resistance using a Zahner Electrik IM6 impedance analyzer over a frequency range of 1 mHz to 100 kHz with an amplitude of 10 mV. The ionic conductivity (σ) was calculated from the impedance data, using the relation $\sigma = t/R_bA$, where t and A are the thickness and area of the composite gel electrolyte, and R_b was bulk resistance measured from the AC impedance spectrum. The lithium transference number was measured at 25°C by a combination of AC impedance and DC polarization methods.[23] The interfacial stability of the lithium and electrolyte under dynamic conditions was investigated by lithium stripping and deposition using a symmetrical Li/electrolyte/Li cell. The symmetrical cell was cycled using a battery test system (WBCS 3000, Wonatech) with a current density of 0.05 to 1.0 mA cm^{-2} at ambient temperature. Charge and discharge cycling tests of the $Li/LiNi_{0.5}Mn_{1.5}O_4$ cells were conducted at a 0.5C rate (0.8 mAh cm^{-2}) over a voltage range of 3.5–4.9 V at 25 and 55°C using battery testing equipment. After the charge-discharge cycling, the lithium negative electrode and $LiNi_{0.5}Mn_{1.5}O_4$ positive electrode were carefully separated from the cell and washed with highly purified EMC to remove residual electrolyte. Both electrodes were then dried under vacuum at 25°C for 12 h. To prevent contamination, the lithium electrode was hermetically sealed inside an aluminum plastic bag for safe transfer to the SEM. Energy dispersive X-ray spectroscopy (EDX) analysis was performed to investigate the quantity of transition metals deposited on the lithium electrode. Powder X-ray diffraction (XRD) (Rigaku, Rint-2000) using Cu-Kα radiation was used to identify the crystalline phase of the cycled $LiNi_{0.5}Mn_{1.5}O_4$ electrodes. HF content in the electrolyte was measured by a neutralization titration method after the cell was stored in a 55°C oven for 5 days.[19] Methyl orange was used as an acid-base indicator.

Results and Discussion

The SiO_2 particles synthesized had uniform spherical shapes with an average diameter of 260 nm, as can be seen in Fig. 1a. The presence of vinyl groups on the silica particle was confirmed by two sharp peaks at 1410 and 1603 cm^{-1} in its FT-IR spectrum (Fig. 1b), which correspond to the characteristic peaks of C=C double bonds. Core-shell structured SiO_2 particles containing poly(sodium acrylate) in the shell were obtained by radical polymerization of vinyl-functionalized silica core particles and sodium acrylate monomer. The Na^+ ions in poly(sodium acrylate) were replaced with Li^+ ions by ion exchange. Fig. 1c shows a TEM image of core-shell structured SiO_2 particles containing a poly(lithium acrylate) shell. The particle has a uniform core-shell morphology with a 170-nm-thick shell layer of poly(lithium acrylate) surrounding a silica core particle. This result implies that the spherical silica particle is encapsulated by poly(lithium acrylate) with a uniform thickness.

A composite gel electrolyte was prepared by soaking the composite polymer membrane, composed of P(VdF-co-HFP) and core-shell structured $SiO_2(Li^+)$ particles, in liquid electrolyte. The electrolyte uptake and ionic conductivities of the different electrolytes (i.e., PP separator with liquid electrolyte, gel electrolyte without $SiO_2(Li^+)$, composite gel electrolyte with SiO_2, composite gel electrolyte with $SiO_2(Li^+)$) are compared Fig. 2a. The PP separator showed low electrolyte uptake due to its inherent hydrophobic properties.[24] The composite gel electrolyte prepared with P(VdF-co-HFP) and fumed SiO_2 exhibited higher electrolyte uptake, since the fumed silica has a high adsorption capability to hold organic solvents. The electrolyte uptake was further increased with addition of $SiO_2(Li^+)$ particles because the carboxylate group in the shell was compatible with the

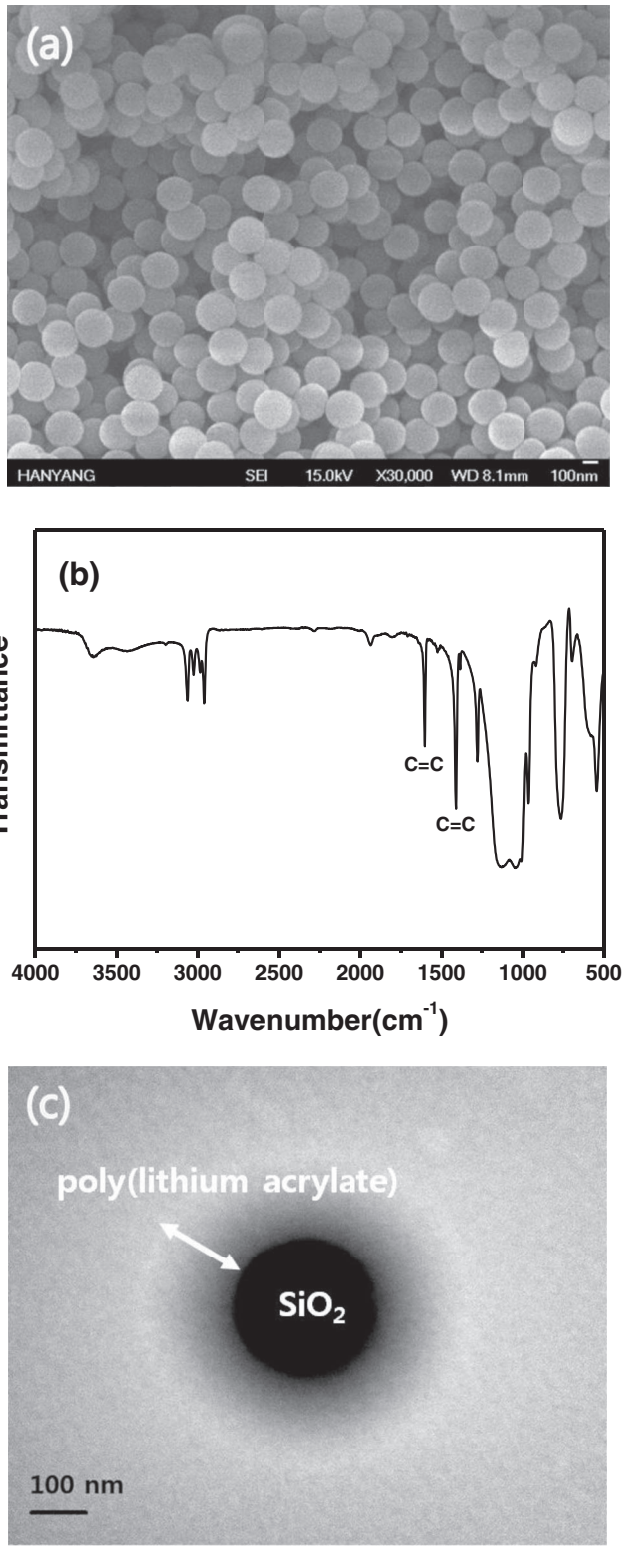

Figure 1. (a) SEM image of vinyl-functionalized SiO_2 core particles, (b) FT-IR spectrum of vinyl-functionalized SiO_2 core particles, and (c) TEM image of a core-shell structured $SiO_2(Li^+)$ particle.

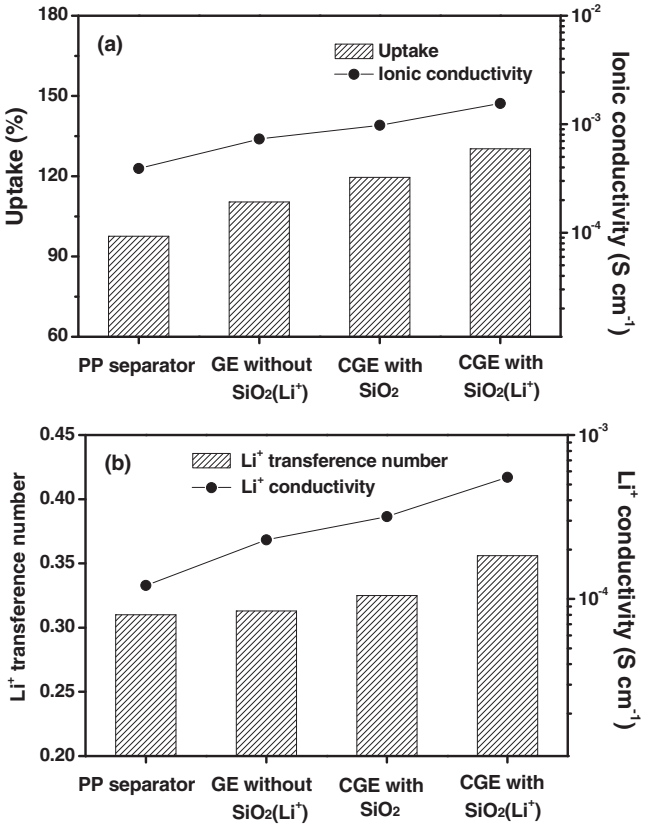

Figure 2. (a) Electrolyte uptake and ionic conductivities of different electrolytes, and (b) lithium transference number and lithium ion conductivities of different electrolytes. GE indicates gel electrolyte without $SiO_2(Li^+)$ particles, and CGE refers to a composite gel electrolyte with fumed SiO_2 or $SiO_2(Li^+)$ particles.

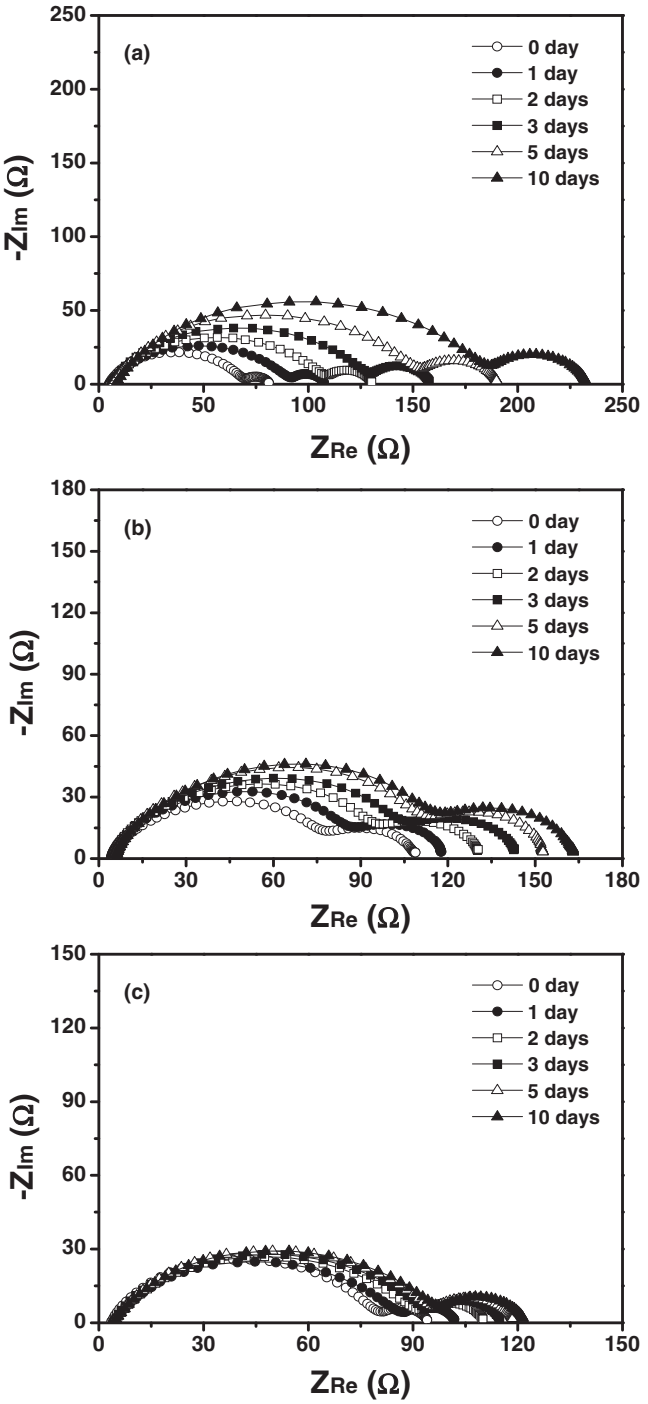

Figure 3. AC impedance spectra of the Li/electrolyte/Li cells with different electrolytes: (a) liquid electrolyte, (b) polymer electrolyte without $SiO_2(Li^+)$, and (c) composite gel electrolyte with $SiO_2(Li^+)$.

carbonate-based liquid electrolyte. Unlike PP separator, the composite gel electrolytes prepared with fumed SiO_2 or $SiO_2(Li^+)$ effectively encapsulated the electrolyte solution without solvent leakage. The ionic conductivity of the composite gel electrolyte with 4 wt% $SiO_2(Li^+)$ particles was 1.55 mS cm^{-1}, which was higher than those observed for the PP separator soaked with liquid electrolyte (0.39 mS cm^{-1}) and the composite gel electrolyte with fumed SiO_2 (0.98 mS cm^{-1}). This increased ionic conductivity was attributed to both the enhanced electrolyte uptake and the increase in mobile lithium ions dissociating from poly(lithium acrylate) in the shell of the $SiO_2(Li^+)$ particles. Indeed, it was confirmed that the lithium transference number increased by adding $SiO_2(Li^+)$ particle into the gel electrolyte. As shown in Fig. 2b, the lithium transference number increased from 0.31 for the gel electrolyte without $SiO_2(Li^+)$ to 0.36 when $SiO_2(Li^+)$ was added. Moreover, the transference number in composite gel electrolyte with $SiO_2(Li^+)$ is higher than one measured in composite gel electrolyte with fumed SiO_2. This result is due to the fact that the $SiO_2(Li^+)$ particle is intrinsically single ion conductor and the lithium ions dissociated from the $SiO_2(Li^+)$ particles contribute to the ionic conductivity. As a result, lithium ion conductivity (σ_{Li+}) estimated from ionic conductivity and lithium transference number was the highest in the composite gel electrolyte with $SiO_2(Li^+)$, as depicted in Fig. 2b.

To investigate the interfacial behavior of the lithium electrode in prolonged contact with electrolyte, AC impedance measurements were performed using different electrolytes in a symmetrical Li/electrolyte/Li cell under open-circuit conditions at 25°C. Figs. 3a, 3b and 3c present the time evolution of the AC impedance spectra of the cells with the liquid electrolyte, polymer electrolyte without $SiO_2(Li^+)$ and composite gel electrolyte with 4.0 wt% $SiO_2(Li^+)$, respectively. The spectra are composed of two partially overlapped semicircles in the medium and low frequency regions. The first semicircle is associated with a passivation film that grows on the lithium electrode (R_f), and the low frequency semicircle is related to charge transfer processes at the electrolyte-electrode interface (R_{ct}).[26–28] A passivation layer spontaneously formed on the lithium electrode due to the deleterious surface reactions that occur between the lithium electrode and the electrolyte solution.[29] Thus, the continuous increase in R_f was attributed to the gradual growth of a resistive surface layer on the lithium electrode. Increases in both R_{ct} and R_f suggested that the resistive surface film formed on the lithium electrode hampered

charge transport at the electrode and electrolyte interface. In the cell that employed a composite gel electrolyte, both R_f and R_{ct} initially increased and eventually stabilized. This indicates that the composite polymer electrolyte suppressed deleterious reactions between the lithium electrode and the composite gel electrolyte, because the composite gel electrolyte effectively trapped the electrolyte solution. The interfacial stability may also have been enhanced by the addition of inorganic $SiO_2(Li^+)$ particles, as reported for other composite gel electrolytes using inorganic materials such as SiO_2, Al_2O_3, TiO_2 and $BaTiO_3$.[30–32] The interfacial adhesion between the lithium electrodes and electrolyte may also have been enhanced due to the adhesive nature of the polymer electrolyte, which results in intimate interfacial contact. Overall, the interfacial stability of the lithium electrode was improved by using composite gel electrolyte instead of liquid electrolyte and PP separator.

To further investigate the interfacial behavior between lithium electrode and electrolyte under dynamic conditions, the symmetrical Li/electrolyte/Li cells with different electrolytes were subjected to galvanostatic charge and discharge cycles at current densities from 0.05 to 1.0 mAh cm^{-2}. Fig. 4 shows the voltage profiles of the galvanostatic lithium stripping and deposition tests performed using the three investigated electrolytes in the symmetrical cells. The liquid electrolyte cell exhibited an unstable and high voltage profile due to the increase in overpotential caused by uneven deposition and stripping of lithium during charge and discharge cycles. Due to the formation and growth of lithium dendrites in the liquid electrolyte, a fresh lithium metal surface is continuously exposed to the liquid electrolyte resulting in the formation of a new solid electrolyte interphase layer and continuous consumption of the electrolyte solution.[33] It results in high resistance and increased polarization in the cell with liquid electrolyte, particularly at high current density. In contrast, the cells employing polymer electrolytes with and without $SiO_2(Li^+)$ showed lower and more stable voltage profiles. Note that the composite gel electrolyte with $SiO_2(Li^+)$ exhibited the lowest voltage profile at all current densities investigated. Thus, the presence of $SiO_2(Li^+)$ particles can reduce the interfacial resistance and provide a favorable charge transfer reaction between the lithium electrode and the composite gel electrolyte. This result is consistent with previous works showing that the addition of an appropriate amount of inorganic filler is effective in decreasing the electrode interfacial resistance.[30–32,34]

Composite gel electrolyte was used to assemble the lithium polymer cell composed of a lithium negative electrode and a $LiNi_{0.5}Mn_{1.5}O_4$ positive electrode. Fig. 5a shows the typical charge and discharge curves of the Li/$LiNi_{0.5}Mn_{1.5}O_4$ polymer cell assembled with a composite gel electrolyte containing 4 wt% $SiO_2(Li^+)$ particles. The cell delivered an initial discharge capacity of 136.6 mAh g^{-1} based on the active $LiNi_{0.5}Mn_{1.5}O_4$ material in the positive electrode. Although the overpotential increased and the reversible capacity decreased with cycling, the cell showed very stable cycling behavior. Fig. 5b shows the discharge capacities of the Li/$LiNi_{0.5}Mn_{1.5}O_4$ cells assembled with different electrolytes as a function of cycle number. The cell with the composite gel electrolyte exhibited a slightly higher initial discharge capacity and better capacity retention than the cells with liquid electrolyte or polymer electrolyte without $SiO_2(Li^+)$ particles. As discussed earlier, the lithium ionic conductivity is the highest and the interfacial resistance is the lowest in the cell employing the composite gel electrolyte with 4 wt% $SiO_2(Li^+)$ particles, which gives a higher discharge capacity. The hydrophilic poly(lithium acrylate) in the shell of the $SiO_2(Li^+)$ particles holds the organic solvent more effectively. This helps to prevent the release of the electrolyte solution which is highly reactive toward lithium metal, resulting in decreased deleterious reaction with lithium electrode and good cycling stability. The enhancement of interfacial stability promoted by the $SiO_2(Li^+)$ particle may also have contributed to the improved capacity retention. On the other hand, the cell assembled with liquid electrolyte showed a significant capacity fading after 120 cycles. The capacity decline observed for rechargeable lithium metal batteries is mainly associated with dendrite formation and exhaustion of the liquid electrolyte.[33] The formation of lithium dendrites exposes fresh Li metal surfaces to

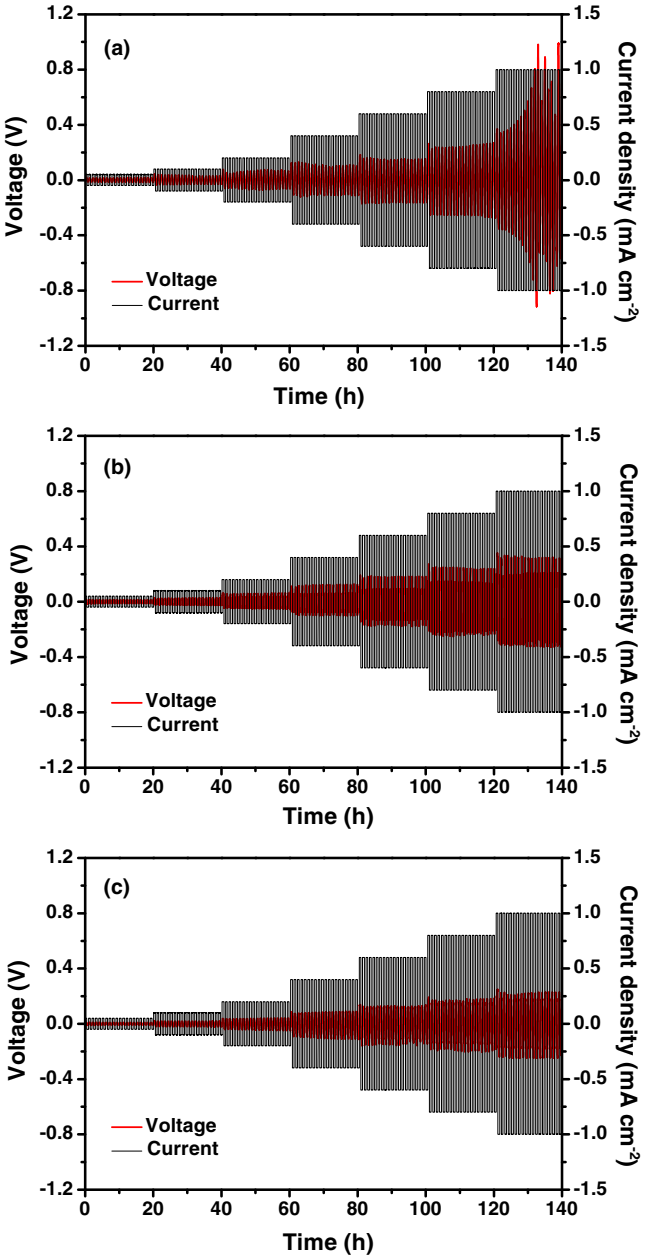

Figure 4. Voltage profiles of the Li/electrolyte/Li cells with increasing current density from 0.05 to 1.0 mAh cm^{-2} for different electrolytes: (a) liquid electrolyte, (b) polymer electrolyte without $SiO_2(Li^+)$, and (c) composite gel electrolyte with $SiO_2(Li^+)$.

the electrolyte and thus, additional resistive layers are continuously generated with gradual consumption of the electrolyte solution. Moreover, lithium dendrites can become isolated from the lithium electrode during repeated cycling. The isolated lithium can then react with the organic electrolyte due to its highly reactive nature, severely degrading the cycling performance.

SEM analysis of the lithium negative electrodes was performed after 100 cycles. As shown in Fig. 6, the SEM images of the lithium electrode surfaces showed significant differences between the types of electrolyte used. The lithium electrode cycled in the liquid electrolyte had dendritic features with particulates. In the liquid electrolyte-based cell, the hydrophobic PP separator showed poor wettability toward the hydrophilic carbonate solution, leading to uneven distribution of Li^+ ions. The interfacial overpotential was thus enhanced at the tip of the lithium dendrite due to its coupling to the local electric field. Because

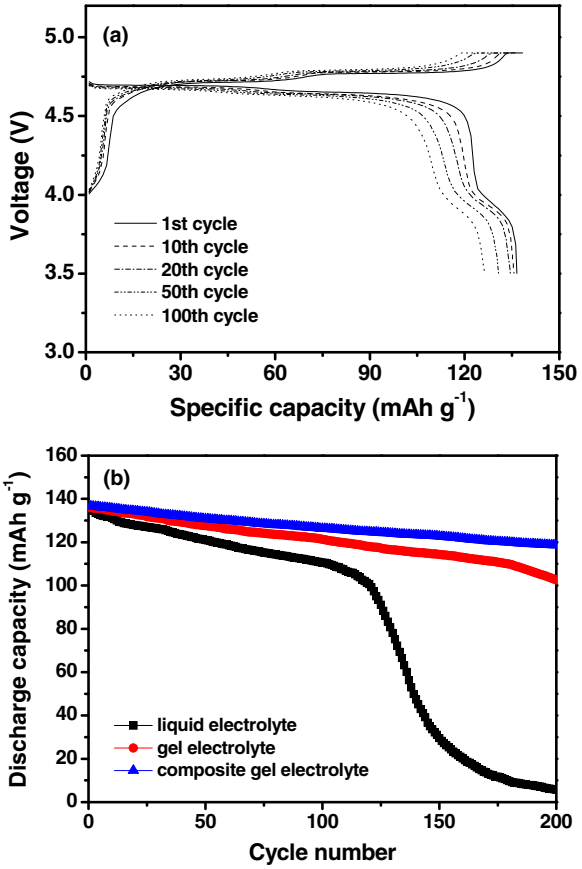

Figure 5. (a) Charge and discharge curves of the Li/$LiNi_{0.5}Mn_{1.5}O_4$ cell assembled with composite gel electrolyte containing 4 wt% $SiO_2(Li^+)$ particles at 25°C (0.5C CC and CV charge, 0.5C CC discharge, cutoff : 3.5–4.9 V). (b) Discharge capacities of the Li/$LiNi_{0.5}Mn_{1.5}O_4$ cells assembled with different electrolytes.

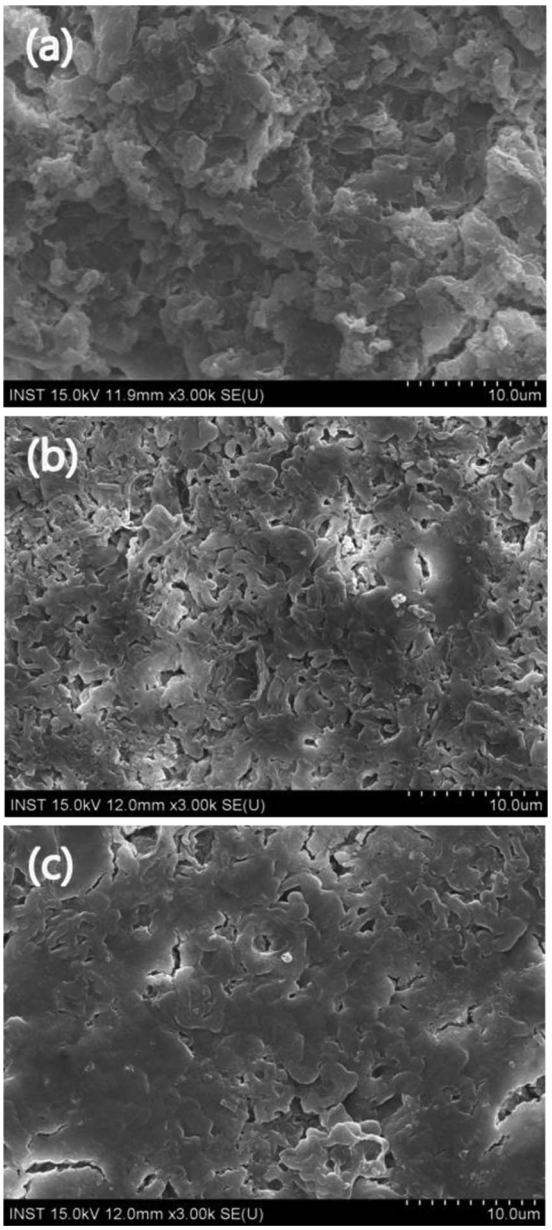

Figure 6. SEM images of lithium electrodes obtained after 100 cycles in different electrolytes at 25°C: (a) liquid electrolyte, (b) polymer electrolyte without $SiO_2(Li^+)$, and (c) composite gel electrolyte with $SiO_2(Li^+)$.

of the inhomogeneous electric field distribution, the dendrite tips experienced increased deposition rates, which further promoted dendrite growth.[35] Therefore, the lithium ions in the liquid electrolyte with a PP separator were unevenly electroplated onto the lithium metal surface, which gave rise to the formation and growth of lithium dendrites. In contrast, the lithium electrodes cycled in polymer electrolyte with and without $SiO_2(Li^+)$ exhibited rather smooth and flat morphologies, indicating that they were spread uniformly over the entire lithium surface. Growth of the lithium dendrites was mechanically suppressed when $SiO_2(Li^+)$ was added to the polymer electrolyte, which gave the most stable surface morphology. These results suggest that the composite gel electrolyte can help uniformly spread Li^+ ion flux over the surface of the lithium electrode and can mechanically suppress lithium dendrite growth, which result in good cycling stability.

To accelerate capacity fading of the Li/$LiNi_{0.5}Mn_{1.5}O_4$ cells, the cells with different electrolytes were cycled at 55°C and 0.5C rate. Fig. 7a shows the discharge capacities of the cells assembled with different electrolytes as a function of the cycle number. The cell with liquid electrolyte suffered from large capacity fading, resulting in a low discharge capacity of 75.6 mAh g^{-1} at the 100th cycle. In contrast, the cells assembled with polymer electrolytes exhibited good cycling stability during cycling. The capacity retentions of the cells employing polymer electrolyte with and without $SiO_2(Li^+)$ particles were 90.0 and 81.0%, respectively. Previous work has shown that gradual capacity fading of spinel $LiNi_{0.5}Mn_{1.5}O_4$ materials at high temperatures is mainly due to the dissolution of transition metals from the active cathode material by HF attack.[36–38] HF is known to be generated by thermal decomposition and hydrolysis of $LiPF_6$ by trace moisture in the electrolyte solution.[39,40] HF content in the different electrolytes was measured after storing the cells at 55°C for 5 days, and the results are shown in Fig. 7b. It can be seen that HF content is the lowest in the composite gel electrolyte containing $SiO_2(Li^+)$. The SiO_2 particles in the composite gel electrolyte served as HF scavengers to remove HF in the electrolyte by the formation of strong chemical bonds via nucleophilic substitution reactions of HF.[22,41] In addition, the oxygen atoms on poly(lithium acrylate) in the shell of the $SiO_2(Li^+)$ particles can effectively complex with the reactive PF_5, which prevents PF_5 from being hydrolyzed to produce HF. Accordingly, the use of composite gel electrolyte containing $SiO_2(Li^+)$ particles reduced HF content and effectively suppressed the dissolution of transition metals from the active $LiNi_{0.5}Mn_{1.5}O_4$ material at elevated temperatures.

In order to better understand the cycling behavior of cells with different electrolytes at 55°C, both the lithium negative electrode and the $LiNi_{0.5}Mn_{1.5}O_4$ positive electrode were carefully removed from the cells after 100 cycles at 55°C, and these electrodes were analyzed using EDX and XRD, respectively. Fig. 8a shows the EDX results for

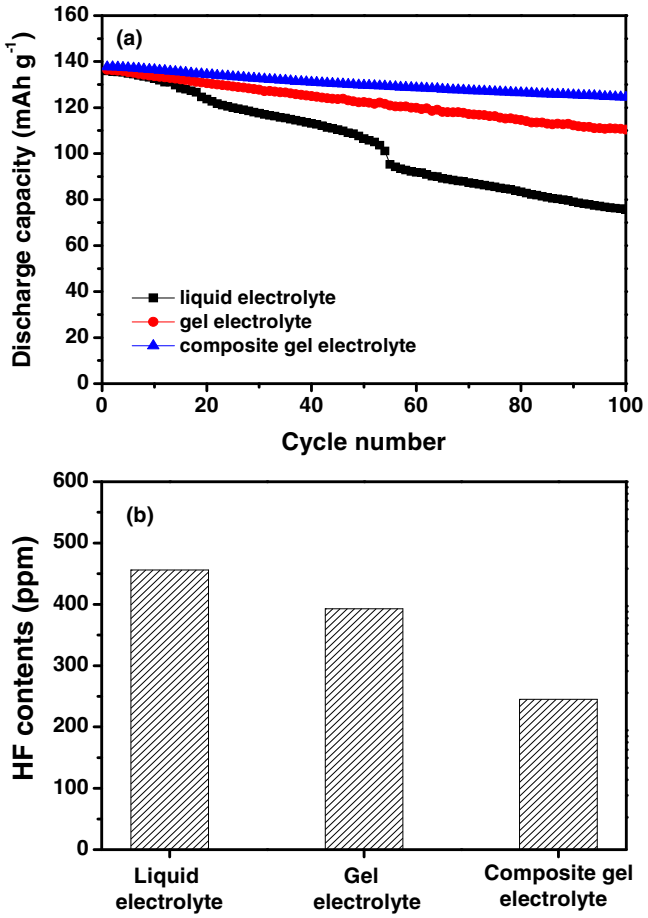

Figure 7. (a) Discharge capacities of the Li/$LiNi_{0.5}Mn_{1.5}O_4$ cells assembled with different electrolytes at 55°C (0.5C CC and CV charge, 0.5C CC discharge, cut-off: 3.5–4.9 V) and (b) HF contents in the different electrolytes after being stored in 55°C oven for 5 days.

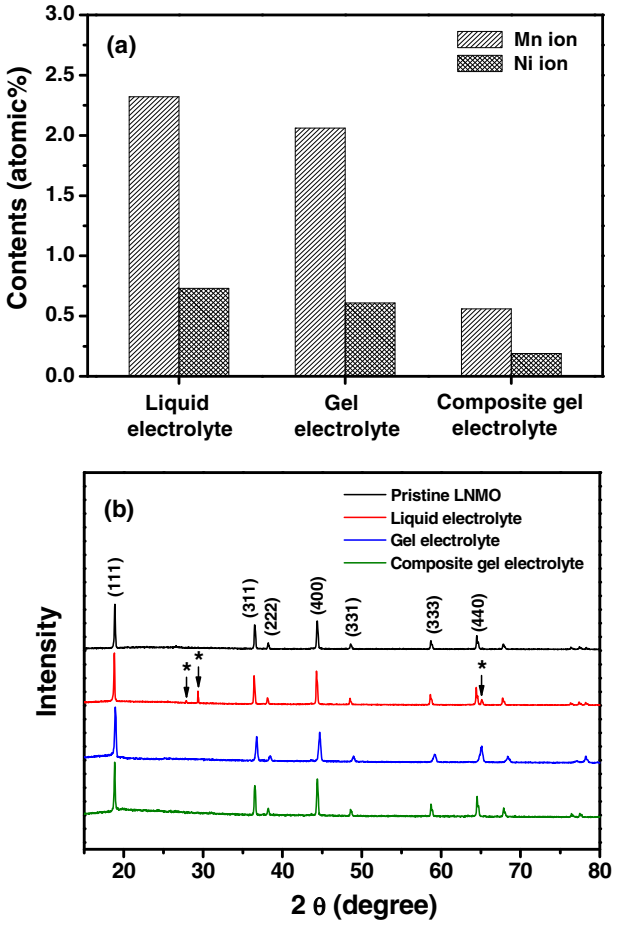

Figure 8. (a) Amount of dissolved Mn and Ni ions deposited on the lithium electrode surface and (b) X-ray diffraction patterns of $LiNi_{0.5}Mn_{1.5}O_4$ electrodes, which were obtained after 100 cycles at 55°C.

the lithium electrode cycled in different electrolytes. These data show that the amount of dissolved Mn and Ni are dependent on the type of electrolyte. The lithium electrode cycled in liquid electrolyte showed higher deposition of Mn and Ni ions after cycling, whereas smaller amounts of Mn and Ni were detected on the surface of the lithium electrode cycled in the polymer electrolytes. Depositions of Mn and Ni on the lithium electrode were significantly reduced with the addition of 4 wt% $SiO_2(Li^+)$ particles. This is due to the presence of SiO_2 particles that reduce HF content according to the mechanism mentioned above. Therefore, the use of composite gel electrolyte containing $SiO_2(Li^+)$ particles was effective in suppressing the dissolution of Mn and Ni by HF attack. The XRD patterns of the $LiNi_{0.5}Mn_{1.5}O_4$ electrodes (pristine and cycled in different electrolytes) are compared in Fig. 8b. The diffraction pattern of the pristine $LiNi_{0.5}Mn_{1.5}O_4$ electrode corresponds to a well-defined spinel structure.[42,43] For the $LiNi_{0.5}Mn_{1.5}O_4$ electrodes cycled in liquid electrolyte, some of the $LiNi_{0.5}Mn_{1.5}O_4$ particles irreversibly transformed to the Li_2MnO_3 rock salt phase. Sun et al. have reported that the degradation mechanism of the spinel electrode at elevated temperature was attributed to the formation of rock salt Li_2MnO_3 resulting from the Mn dissolution due to HF presence in the electrolyte.[19] Therefore, it is important to reduce HF content in order to maintain the structural stability at high temperature. On the other hand, the diffraction patterns of $LiNi_{0.5}Mn_{1.5}O_4$ electrodes cycled in polymer electrolytes were almost the same as those observed for the pristine electrode, confirming that there are no structural transformations from the parent spinel to an inactive phase during high temperature cycling. This result suggests that the use of a composite gel electrolyte effectively reduces HF content, as explained above, resulting in improvement of structural stability at 55°C. Thus, the structural stability of $LiNi_{0.5}Mn_{1.5}O_4$ active materials led to better cycling stability in the cells employing the composite gel electrolyte at elevated temperatures.

Conclusions

Composite gel electrolyte was prepared using core-shell structured SiO_2 particles containing poly(lithium acrylate), and its electrochemical properties were characterized. The composite gel electrolyte effectively encapsulated an electrolyte solution without solvent leakage, exhibited high ionic conductivity and showed favorable interfacial characteristics at the lithium electrode. The lithium polymer cell employing the composite gel electrolyte composed of a lithium negative electrode and a $LiNi_{0.5}Mn_{1.5}O_4$ positive electrode delivered a high discharge capacity and exhibited good capacity retention. SEM, EDX and XRD analysis of the electrodes revealed that the growth of lithium dendrites and the dissolution of transition metals were effectively suppressed by the composite gel electrolytes during cycling.

Acknowledgments

This work was supported by the Basic Science Research Program of the National Research Foundation of Korea (NRF), funded by the Ministry of Science, ICT and Future Planning (2014R1A2A2A01002154) and the R&D Convergence Program of the NST (National Research Council of Science & Technology) of the Republic of Korea.

References

1. J. M. Tarascon and M. Armand, *Nature*, **414**, 359 (2001).
2. R. Bhattacharyya, B. Key, H. Chen, A. S. Best, A. F. Hollenkamp, and C. P. Grey, *Nat. Mater.*, **9**, 504 (2010).
3. S. Chandrashekar, N. M. Trease, H. J. Chang, L. Du, C. P. Grey, and A. Jerschow, *Nat. Mater.*, **11**, 311 (2012).
4. S. Tobishima and J. Yamaki, *J. Power Sources*, **81–82**, 882 (1999).
5. D. Fenton, J. Parker, and P. Wright, *Polymer*, **14**, 589 (1973).
6. M. B. Armand, *Solid State Ionics*, **69**, 309 (1994).
7. A. S. Arico, P. Bruce, B. Scrosati, J. M. Tarascon, and W. Van Schalkwijk, *Nat. Mater.*, **4**, 366 (2005).
8. J. Y. Song, Y. Y. Wang, and C. C. Wan, *J. Power Sources*, **77**, 183 (1999).
9. M. Marcinek, J. Syzdek, M. Marczewski, M. Piszcz, L. Niedzicki, M. Kalita, A. Plewa-Marczewska, A. Bitner, P. Wieczorek, T. Trzeciak, M. Kasprzyk, P. Lezak, Z. Zukowska, A. Zalewska, and W. Wieczorek, *Solid State Ionics*, **276**, 107 (2015).
10. S. M. Park, Y. S. Lee, and D. W. Kim, *J. Electrochem. Soc.*, **162**, A3071 (2015).
11. M. S. Whittingham, *Chem. Rev.*, **104**, 4271 (2004).
12. M. Mohamedi, M. Makino, K. Dokko, T. Itoh, and I. Uchida, *Electrochim. Acta*, **48**, 79 (2002).
13. Y. Shin and A. Manthiram, *Electrochim. Acta*, **48**, 3583 (2003).
14. S. Patoux, L. Daniel, C. Bourbon, H. Lignier, C. Pagano, F. L. Cras, S. Jouanneau, and S. Martinet, *J. Power Sources*, **189**, 344 (2009).
15. Y. Sun, Y. Yang, H. Zhan, H. Shao, and Y. Zhou, *J. Power Sources*, **195**, 4322 (2010).
16. V. Borgel, E. Markevich, D. Aurbach, G. Semrau, and M. Schmidt, *J. Power Sources*, **189**, 331 (2009).
17. S. Y. Bae, W. K. Shin, and D. W. Kim, *Electrochim. Acta*, **125**, 497 (2014).
18. Y. Kobayashi, H. Miyashiro, K. Takei, H. Shigemura, M. Tabuchi, H. Kageyama, and T. Iwahori, *J. Electrochem. Soc.*, **150**, A1577 (2003).
19. Y. K Sun, K. J. Hong, J. Prakash, and K. Amine, *Electrochem. Commun.* **4**, 344 (2002).
20. H. B. Kang, S. T. Myung, K. Amine, S. M. Lee, and Y. K. Sun, *J. Power Sources*, **195**, 2023 (2010).
21. W. K. Shin, Y. S. Lee, and D. W. Kim, *J. Mater. Chem. A*, **2**, 6863 (2014).
22. W. Cho, S. M. Kim, J. H. Song, T. Yim, S. G. Woo, K. W. Lee, J. S. Kim, and Y. J. Kim, *J. Power Sources*, **282**, 45 (2015).
23. J. Evance, C. A. Vincent, and P. G. Bruce, *Polymer*, **28**, 2324 (1987).
24. H. Lee, M. Yanilmaz, O. Toprakci, K. Fu, and X. Zhang, *Energy Environ. Sci.*, **7**, 3857 (2014).
25. D. W. Kim and Y. K. Sun, *J. Electrochem. Soc.*, **145**, 1958 (1998).
26. G. B. Appetecchi, F. Croce, G. Dautzenberg, M. Mastragostino, F. Ronci, B. Scrosati, F. Soavi, A. Zanelli, F. Alessandrini, and P. P. Prosini, *J. Electrochem. Soc.*, **145**, 4126 (1998).
27. S. Liu, N. Imanishi, T. Zhang, A. Hirano, Y. Takeda, O. Yamamoto, and J. Yang, *J. Electrochem. Soc.*, **157**, A1092 (2010).
28. S. M. Choi, I. S. Kang, Y. K. Sun, J. H. Song, S. M. Chung, and D. W. Kim, *J. Power Sources*, **244**, 363 (2013).
29. C. H. Chen, J. Liu, and K. Amine, *J. Power Sources*, **96**, 321 (2001).
30. F. Croce and B. Scrosati, *J. Power Sources*, **43**, 9 (1993).
31. M. C. Borghini, M. Mastragostino, S. Passerini, and B. Scrosati, *J. Electrochem. Soc.*, **142**, 2118 (1995).
32. F. Croce, G. B. Appetecchi, L. Persi, and B. Scrosati, *Nature*, **394**, 456 (1998).
33. D. Aurbach, E. Zinigrad, Y. Cohen, and H. Teller, *Solid State Ionics*, **148**, 405 (2002).
34. S. Srivastava, J. L. Schaefer, Z. Yang, Z. Tu, and L. A. Archer, *Adv. Mater.*, **26**, 201 (2014).
35. Z. Li, J. Huang, B. Yann Liaw, V. Metzler, and J. Zhang, *J. Power Sources*, **254**, 168 (2014).
36. J. Arrebola, A. Caballero, L. Hernan, J. Morales, E. R. Castellon, and J. R. R. Barrado, *J. Electrochem. Soc.*, **154**, A178 (2007).
37. J. Liu and A. Manthiram, *J. Electrochem. Soc.*, **156**, A66 (2009).
38. D. J. Lee, K. S. Lee, S. T. Myung, H. Yashiro, and Y. K. Sun, *J. Power Sources*, **196**, 1353 (2011).
39. H. Yang, G. V. Zhuang, and P. N. Ross Jr., *J. Power Sources*, **161**, 573 (2006).
40. S. F. Lux, I. T. Lucas, E. Pollak, S. Passerini, M. Winter, and R. Kostecki, *Electrochem. Commun.*, **14**, 47 (2012).
41. T. Yim, H. J. Ha, M. S. Park, K. J. Kim, J. S. Yu, and Y. J. Kim, *RSC Adv.*, **3**, 25657 (2013).
42. J. Gao, J. Li, C. Jiang, and C. Wan, *J. Electrochem. Soc.*, **157**, A899 (2010).
43. X. Huang, Q. Zhang, J. Gan, H. Chang, and Y. Yang, *J. Electrochem. Soc.*, **158**, A139 (2011).